Hybrid synthesis of fluid structure interaction by non-linear feedback control strategy for characterizing steam generators tubes subjected to impacts

W.Benmalek[1&2], M.Collet[2], E.Foltete[2], M.Ouisse[2], M.Corus[1]
[1] Electricité de France R&D,
1, avenue du général de gaulle, 92141 Clamart, France
e-mail: **wissam.benmalek@femto-st.fr**

[2] FEMTO-ST Institute, Applied Mechanics Department
24, rue de l'épitaphe, 25000 Besançon, France

Abstract
In steam generators, the primary loop tubes are subjected to fluid coupling forces and impacts. Understanding the behavior of these tubes is crucial when designing steam generators. In fact, mastering aforementioned could allow engineers to improve the design of these components optimizing the safety factors and ameliorating the overall performances and the average life of the structure.

The aim of our research is to provide a better understanding of the conjugate effects of impacts and coupling with fluid-elastic forces on the system's stability. Since fluid-elastic forces are difficult to simulate and expensive to reproduce experimentally, the fluid coupling forces of our numerical model are represented using velocity dependent damping and stiffness matrices, both for the fluid and the tube.

In this paper, first we present a hybrid approach consisting on determining experimentally both the modal contribution of fluid-elastic forces and impact forces to feed our semi-analytical model. Then an active vibration control approach is setup to reproduce the modal contribution of fluid-elastic forces on the tube taking in consideration the non-linearities due to the impacts.

1 Introduction

Steam generators are heat exchangers used to convert water into steam from heat produced in a nuclear reactor core. They are used in pressurized water reactors between the primary and secondary coolant loops.

When the steam generator is operating, water in the secondary loop partially changes to steam. When rising up, this fluid interacts with the U-tubes (figure 1), which are therefore subjected to flow excitation.

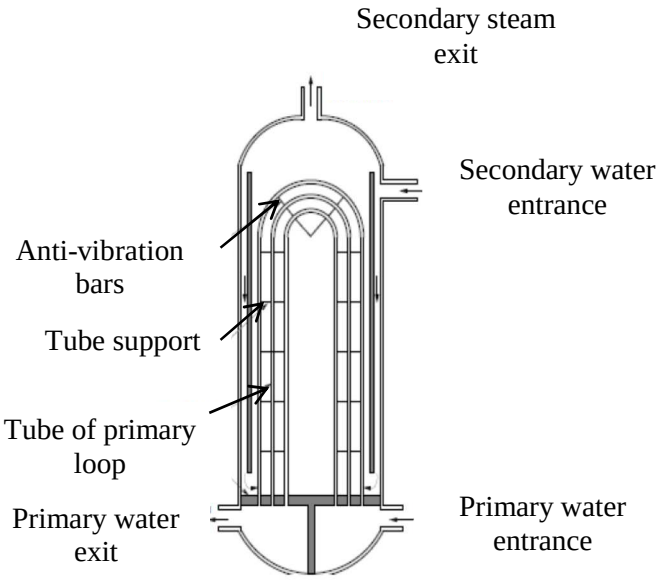

Figure 1: Steam generator

This excitation can be split into two kinds of forces: turbulence forces F_T which are independent of the movement of the tube and the so-called fluid-elastic coupling forces F_{f-e}, depending on acceleration, velocity, displacement and fluid reduced velocity Vr [1], [2]. The total flow excitation can be finally expressed as:

$$F_T + F_{f-e}(\ddot{y}, \dot{y}, y, Vr) = F_T - M_f.\ddot{y} - C_f(Vr).\dot{y} - K_f(Vr).y \quad (1)$$
$$V_r = V/(Df)$$

Where $\ddot{y}, \dot{y}$ and y are acceleration, velocity and displacement vectors, M_f added masse, C_f added damping and K_f added stiffness. These last two coefficients are assumed depending on V_r. Under some specific conditions of fluid reduced velocity V_r [1], C_f is negative enough to make the structure instable. This phenomenon is called fluid-elastic instability and can damage the structure. The tubes are however supported by plates (figure 1) which guide them and limit their vibration amplitude. In fact, the impacts between the tubes and the plate tend to stabilize the tubes. Thus, we can finally represent the whole problem as below:

$$\mathcal{M} \cdot \ddot{y} + \mathcal{C} \cdot \dot{y} + \mathcal{K} \cdot y = F_t + F_{f-e}(\ddot{y}, \dot{y}, y, V_r) + F_c \quad (2)$$

Where $\mathcal{M}$, $\mathcal{C}$ and $\mathcal{K}$ are structural mass matrix, structural damping matrix and structural stiffness matrix. F_c is the impact force.

Premultiplying the (Eq.2) by modal base Φ we get a set of equations of motion in the modal coordinates.

$$\mathcal{M}_m \cdot \ddot{q} + \mathcal{C}_m \cdot \dot{q} + \mathcal{K}_m \cdot q = f_t + f_{f-e}(\ddot{q}, \dot{q}, q, V_r) + f_c \quad (3)$$

Where $\ddot{q}, \dot{q}, q$ are generalized acceleration, velocity and displacement vectors, and $\mathcal{M}_m$, $\mathcal{C}_m$, $\mathcal{K}_m$ modal mass, damping, stiffness diagonal matrices. Because these mechanisms are complex and difficult to realize in an experimental set up, the main aim of our study is to develop a hybrid control loop to simulate this coupling effect in the frame of an experimental characterization test bench.

2 Structure & modal updating

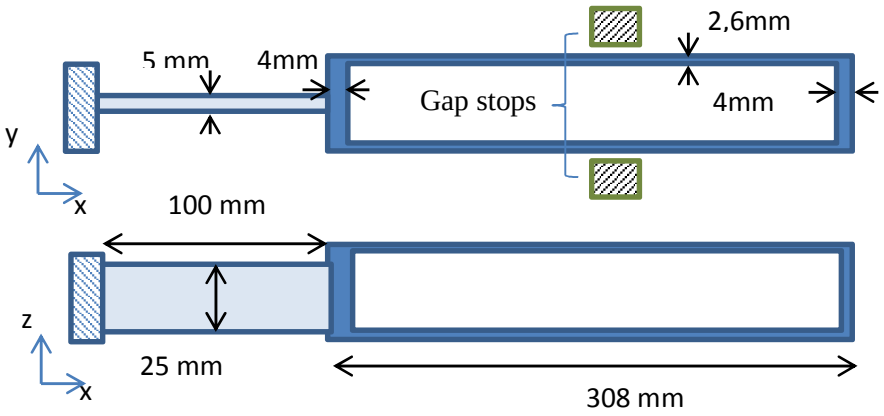

Figure 2: Gap supported tube

The studied structure (figure 2) is composed of a tube attached to a slender plate clamped in rigid block. At the middle height of the tube, two gap stops located at 0.5mm create punctual impacts depending on the tube vibration amplitude.

A finite element shell model was developed to generate the mass, damping and stiffness matrices. This model was updated in order to match the numerical behavior with experimental one. Two criterions were used to compare the numerical and experimental model: Modal Assurance Criterion (MAC) and frequency error criterion. Figure 3 & Table 1 summarizes the results obtained for the 6 first modes.

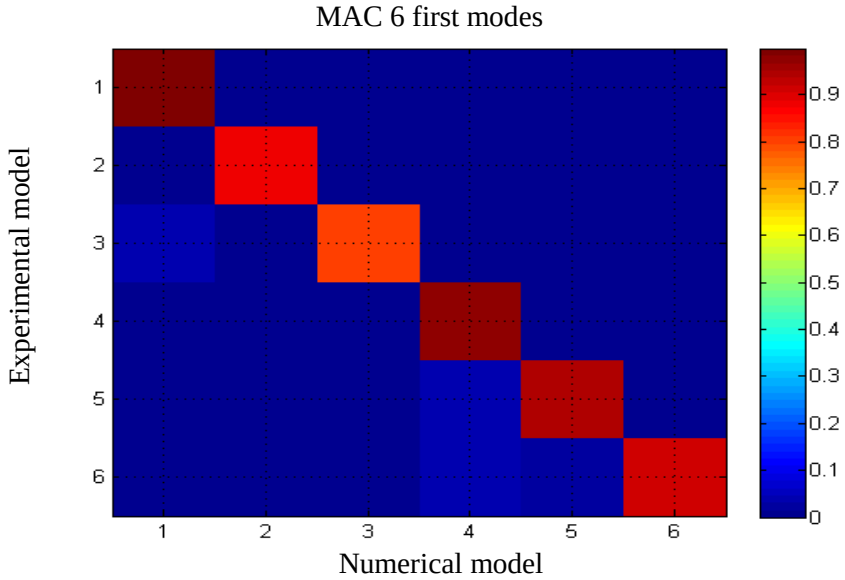

Figure 3: MAC

It can be observed that there is a good agreement between the two models. The lowest value of MAC is 85% and the mean frequency error is lower than 4% (Table 1).

Modes	Numerical modal frequency	Experimental modal frequency	Error %
1	23.1	23	~ 0
2	103	100	3
3	305	318	4
4	426	407	4.6
5	774	798	3
6	1300	1404	8
		Mean	3.7

Table 1: Frequency error

3 Loads parameters identification

3.1 Impact stiffness

The only source of nonlinearity in our problem comes from the impact forces located at x_c (middle height of tube), which are computed in an explicit manner as the (Eq.4) shows.

$$\begin{cases} F_c(t) = -\frac{y_c(t)}{|y_c(t)|} K_c.(|y_c(t)| - g) & if\ |y_c(t)| > g \\ F_c(t) = 0 & if\ |y_c(t)| \leq g \end{cases} \quad (4)$$

Where g is a gap distance, y_c is displacement at loose support and K_c is the impact stiffness. The value of the parameter K_c is identified through experimental measurements. Several impact tests were performed in which the impact forces where measured by using force sensor. Knowing the mass sensor M_c (26.5g) and measuring the duration of the impact Tc, we can deduce an estimation of the impact stiffness using the following approximation:

$$Tc = \frac{\pi}{\omega_c} = \pi\sqrt{M_c/K_c} \quad (5)$$

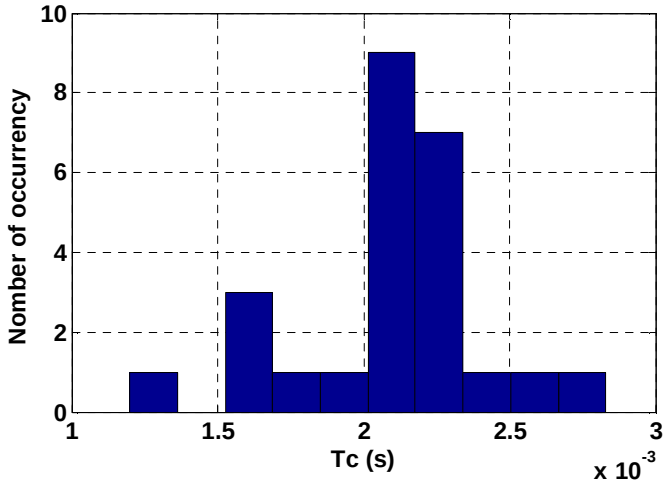

Figure 4: Impact duration

Figure 4 presents a histogram of the obtained results for 25 tests. K_c is estimated at $3 \cdot 10^4 \mathrm{N/m}$ on average (for $T_c = 2\mathrm{ms}$ on average).

3.2 Turbulences excitations

The turbulence forces were modeled by a random signal. Since only the first mode is under fluid-elastic coupling, the turbulence excitation was constructed by creating first a limited spectrum band to 40Hz, than using the Inverse Fast Fourier Transform (IFFT) technic to get the temporal signal. The RMS amplitude was fixed arbitrary to 1. This level will be multiplied by different gains for each fluid velocity. The figure 5 presents a sample of the turbulence signal used in experiments and simulations.

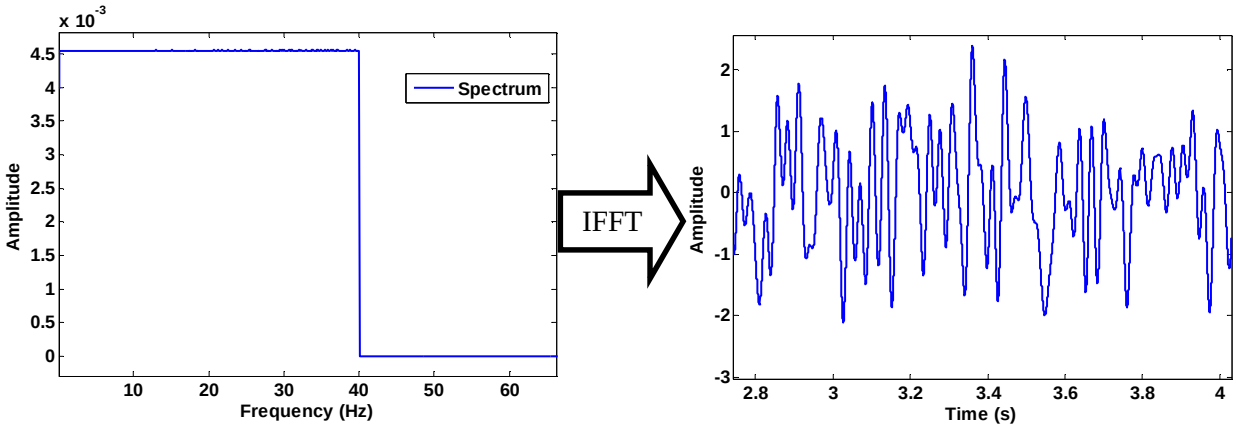

Figure 5: Sample of turbulence forces

3.3 Fluid-elastic coupling coefficients

A significant research effort has been conducted over the last four decades to model fluid-elastic forces. These researches leaded to several theoretical models. We can quote Tanaka [2], M.Paidoussis [3], or Weaver & Lever [4] models etc. In our study we have chosen the CEA one [1] which is semi-analytical model. In this approach, the coupling parameters: M_f, C_f and K_f are identified experimentally to feed the numerical formula (Eq.1). In addition, it has been demonstrated that the first mode is predominant in the tube response and the effects of higher modes are almost negligible, thus the fluid elastic forces were projected only on the first mode and the other modes are not influenced (Eq.6).

$$f_{f.e}(\ddot{q_1}, \dot{q_1}, q_1) = -(m_f \ddot{q_1} + c_f(V_r)\dot{q_1} + k_f(V_r)q_1) \tag{6}$$

To achieve the fluid-elastic forces modeling, the three coupling parameters were identified from the modal characteristics of the structure for each fluid velocity. First we assume that the modal frequency and the modal damping are known in the air, also we suppose the fluid-added mass m_f is independent on fluid velocity. With this last assumption, m_f is identified through the first mode frequency in the air and in the stagnant water ($k_f = 0$) by using formula (Eq.7). Then for each fluid velocity, the parameters k_f and c_f are inferred from the first modal frequency and modal damping by using (Eq.7) and (Eq.8).

$$\omega(V_r) = \sqrt{\frac{k_1 + k_f(V_r)}{m_1 + m_f}} \tag{7}$$

$$\zeta(V_r) = \frac{c_1 + c_f(V_r)}{2\omega(m_1 + m_f)} \tag{8}$$

The figure 7 presents the modal parameters of the coupled system (tube+fluid-elastic) for each fluid velocity.

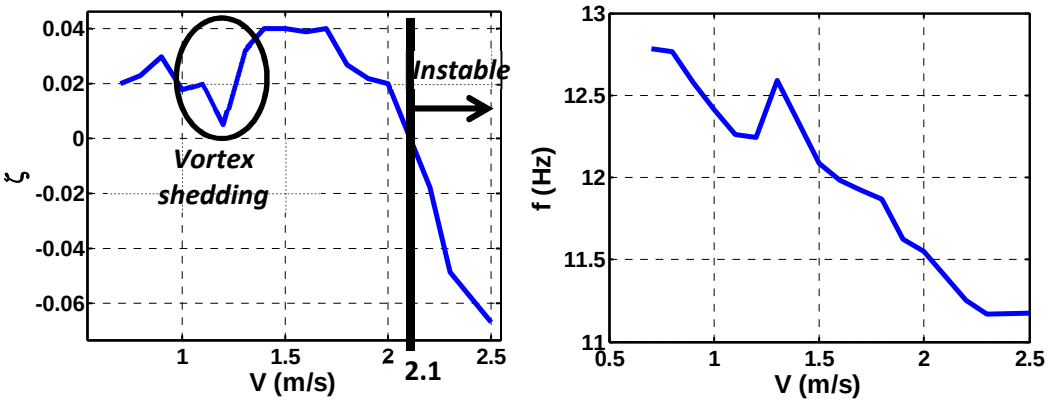

Figure 6: First mode parameters depending on fluid velocity

4 Active control & pole placement

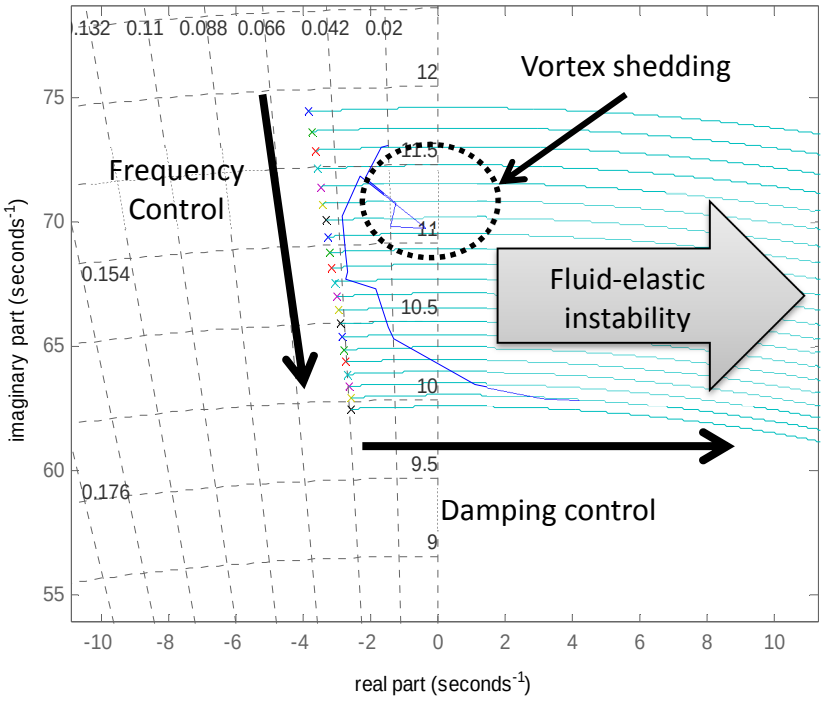

Figure 7: Evolution of the first mode (pole) under fluid-elastic forces

After characterizing all load parameters, the next step is to perform a hybrid test to simulate the modal contribution of fluid-elastic forces on tube dynamics by using active control vibration technics. The modal parameters of figure 6, were reinterpreted in such way to facilitate the controller design. We have chosen root-locus plot, in which we plot the evolution of poles (blue curve) under fluid-elastic effect by using pole equation definition (Eq.7):

$$p_i = -\zeta_i \omega_i \pm j\omega_i \sqrt{(1-\zeta_i^2)} \tag{7}$$

This plot (figure 7) emphasizes the vortex shedding and makes this phenomenon more visible than in figure 6, also we notice that the system becomes instable from a certain velocity when the real part of the associated pole becomes positive.

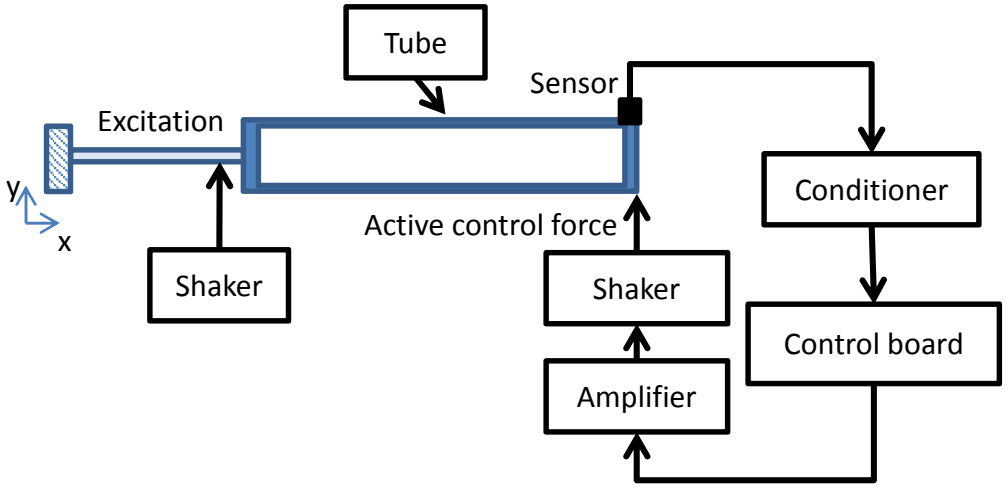

Figure 8: Control loop

In our study, the turbulence excitation is located at the end of slender plate, because the inflexion of the firs mode principally appears at this plate and not on the tube. Concerning the control force, it's applied at the free end of tube, because at this location the quality of measurement over background noise is the best and the structure is flexible so the shaker doesn't need lot of energy to impose the modal contribution corresponding to the fluid-elastic force.

To reproduce the modal parameters of the coupled system, we built 2 controllers: the first one allocates the modal frequency and the second one the modal damping as shown in figure 7. Proceeding in this way, we can cover all the area where the 1st pole of the coupled system is located by just tuning two gains control. The design of these controllers is based on very careful identification of each control loop component (shaker, amplifier, conditioner, tube etc.) and also takes in consideration the spillover problem by filtering the excitation of higher modes. After numerical tests, we identified the gains associated to each fluid velocity in order to fit the modal parameters. The figure 8 displays the hybrid test and numerical pole location in the s-plan. We notice a good agreement between experiments and simulations results, in addition to the ability to reproduce the vortex shedding and fluid-elastic instability with the active control loop.

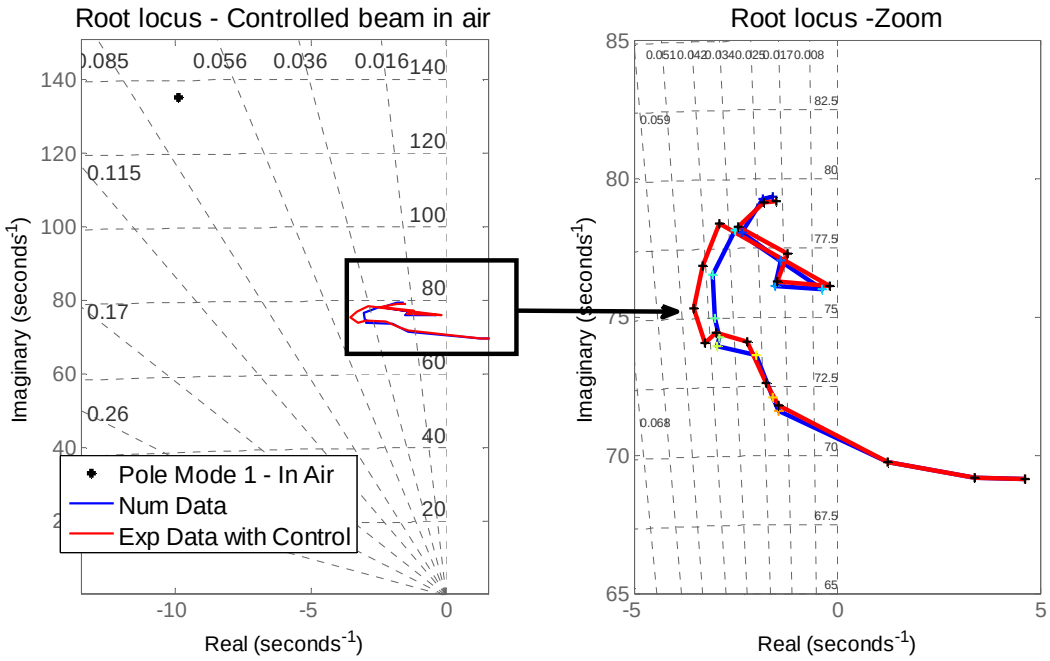

Figure 9: Experimental (tube under active control) VS Numerical results (tube under fluid-elastic effect)

Now that we are able to perform a hybrid test including fluid-elastic force effect in linear case, the next step is to introduce a local non-linearity in our study.

5 Non-linear hybrid test validation

We now address the final aspect of this work, which consists in comparing the experimental and numerical tube dynamics under fluid-elastic effect and impacts. When including impacts in the problem, the expression of the reduced fluid velocity in (Eq.1) becomes a little more complicated, since it depends on vibration *quasi-instantaneous* frequency of tube and not anymore on the first modal frequency as proposed Fricker [5] in his works.

There are different ways for estimating this quasi-instantaneous frequency of the tube's vibration. In this study we have chosen Rice frequency method [6] noted f_{R}, which is proportional to velocity RMS over displacement RMS of the tube free end within sliding size windows τ (Eq.8).

$$f_{\mathrm{R}}(t,\tau) = \frac{\sigma_{\dot{y}}(t,\tau)}{2\pi\sigma_{y}(t,\tau)} \tag{8}$$

Consequently, the new expression of V_r in non-linear study as from now is:

$$V_r = V/(f_{\mathrm{R}} * D) \tag{9}$$

The fluid elastic forces are then updated continuously depending on reduced fluid velocity estimation.

5.1 Experimental setup

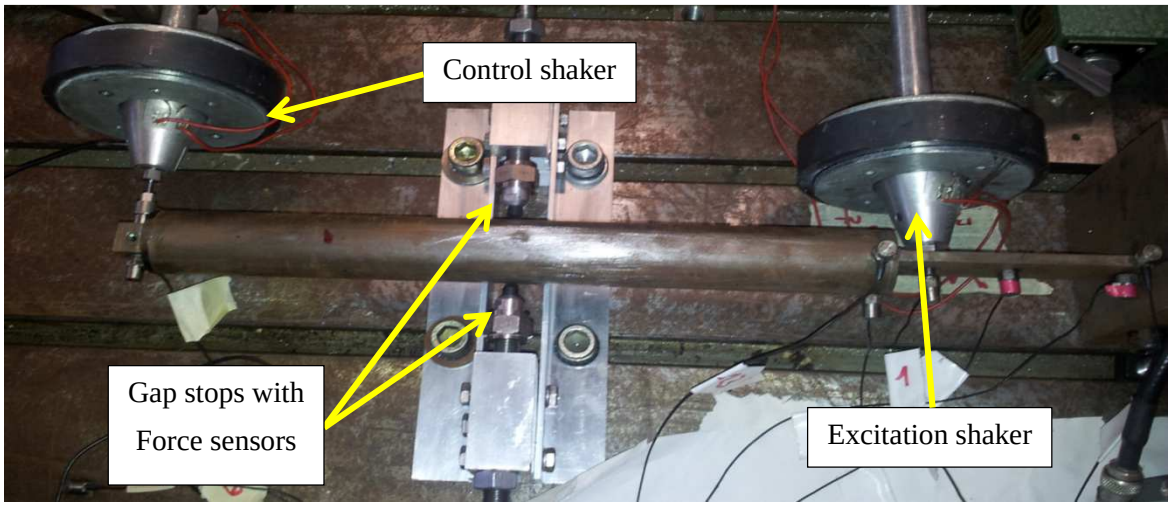

Figure 10: Experimental active control setup

Figure 10 shows the experimental setup of the tube under active control. Two shakers are used, first one is used for turbulence excitation (fixed on flat bar) and the second one is for the control (fixed on the free end of tube), both actuators are oriented in the y direction (direction of interest). In the middle high of the tube are located two gap stops with an integrated force sensor, in order to measure the impact forces. The acceleration sensor used for the control loop is located in the free-end of the tube in order to perform a collocated control. The controller board, where the controllers are implemented, is provided by dSpace. This devise generates the signal command from measured acceleration and send it to the control actuator.

5.2 Results analysis

The direct comparison of the detailed plots is not relevant and results should be compared in a statistical sense, since turbulence forces are modeled by random excitation. Figure 11 compares numerical results to experimental ones. On the left side, a detailed plot of the free end displacement for both numerical simulation and experimental measurement are shown. On the right side, are plotted their associated histograms.

Through the detailed plots we can highlight that the displacement is bounded by the double of the gap distance (gap=0.5mm). This can be apprehended from the first beam mode shape which is the mainly responding under fluid-elastic forces. The histogram distribution is centered on zero, namely the initial equilibrium position. Also we notice a good agreement of the time estimation between computational and experimental responses.

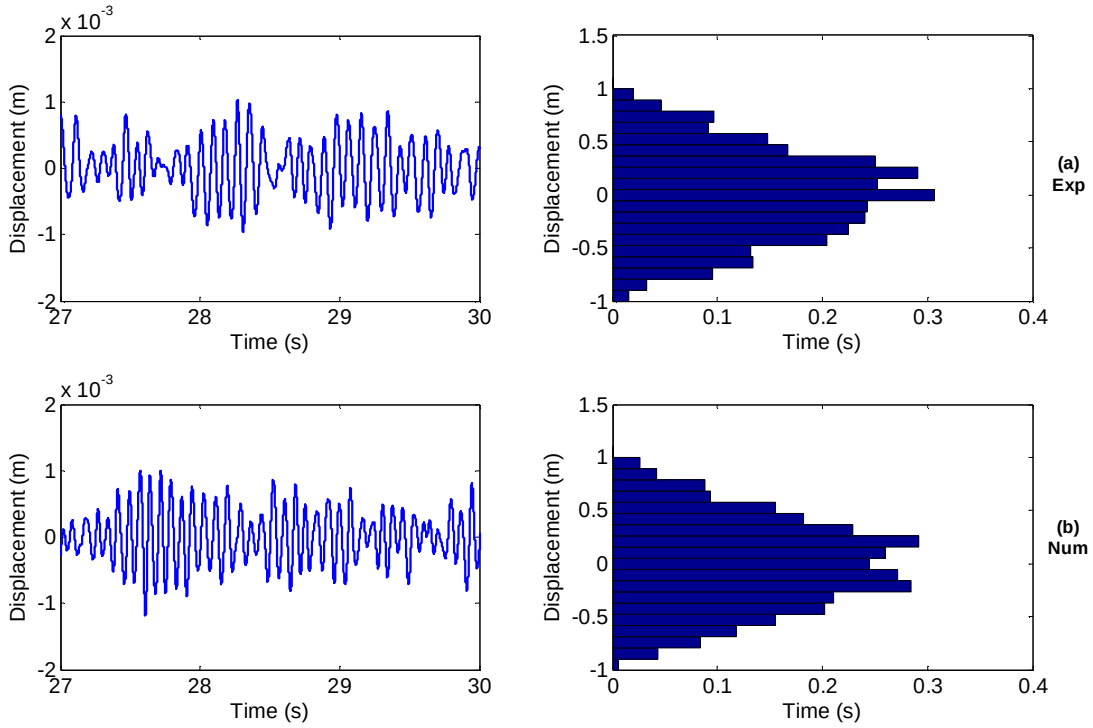

Figure 11: Tube displacement & histogram for V=1.7m/s & Gain excitation=5 (Num VS Exp)

The figure 12 compares the computed and measured impact forces by using a convenient graph “whiskers box”. The box depicts the data through their quartiles; the extended line (whiskers) indicates variability outside the upper and lower quartiles. Finally, outliers data are plotted as individual points and the median value is plotted as red line in the box.

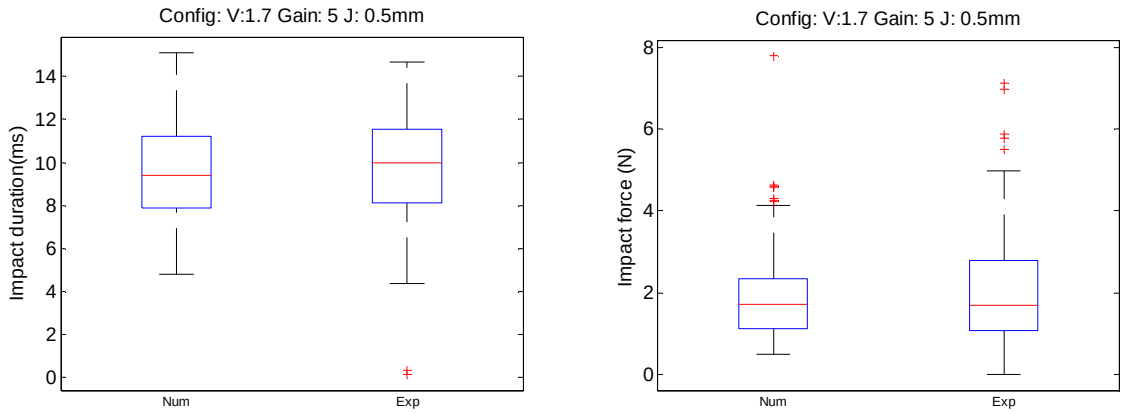

Figure 12: Impact durations and forces for V=1.7m/s and Gain excitation=5 (Num VS Exp)

As figure 12 shows for a first configuration (V=1.7m/s and gain excitation =5), all quartiles of the impact durations and forces are well estimated. The mean duration is about 9.5ms and 9.7ms for numerical and experimental data (Table 2). We have also counted about 118 impacts for numerical simulation against 119 impacts for experiment. Concerning the impact force maxima, we obtained 7.7N for numerical simulation against 7.1N measured. The table 2, summarizes the results and gives calculated relative errors (in percent) between the experimental and numerical results.

	Num	Exp	Err%
Fmax	7,7	7,1	9
Occurrence	118	119	0,8
Mean duration (ms)	9,49	9,7	2

Table 2: Comparison between experimental and numerical results (V=1.7m/s & Gain excitation=5)

Figure 13 & 14 displays results for the second configuration (V=2.5m/s and gain excitation =7). In the detailed plot we still notice that the displacement is bounded at about double of the gap distance as in the first configuration. However, the histogram shows a severe instability of the system with a far-from Gaussian distribution as presented before. Despite of this violent non-linear regime, computational results fits well measured ones.

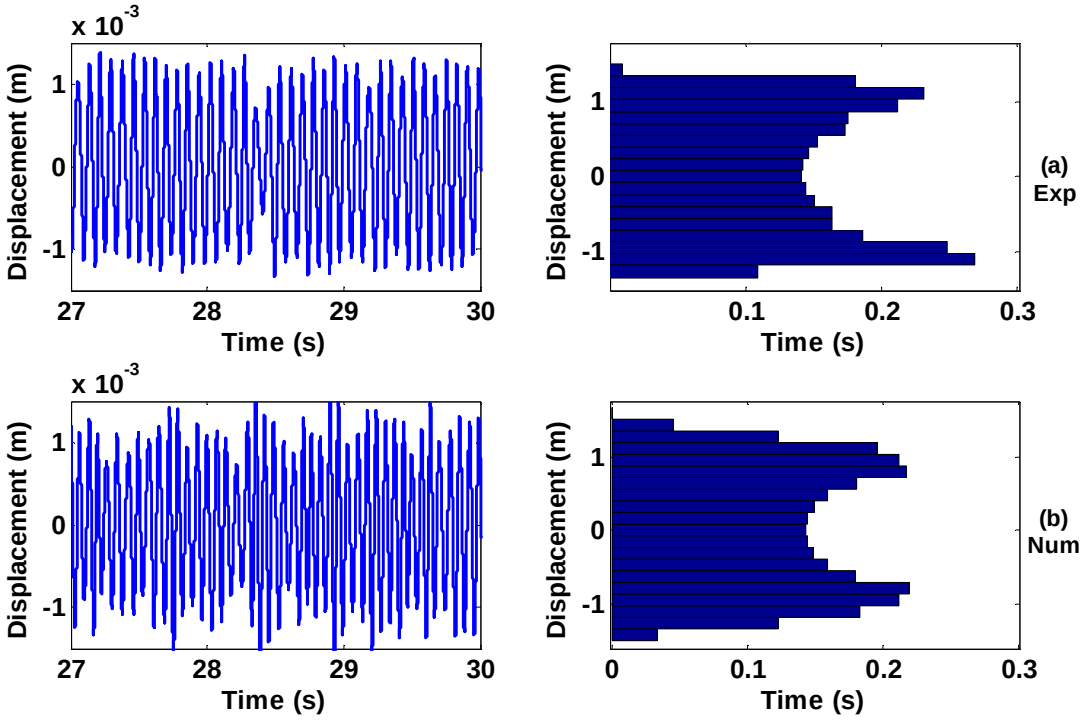

Figure 13: Tube displacement and histogram for V=2.5m/s and Gain excitation=7 (Num VS Exp)

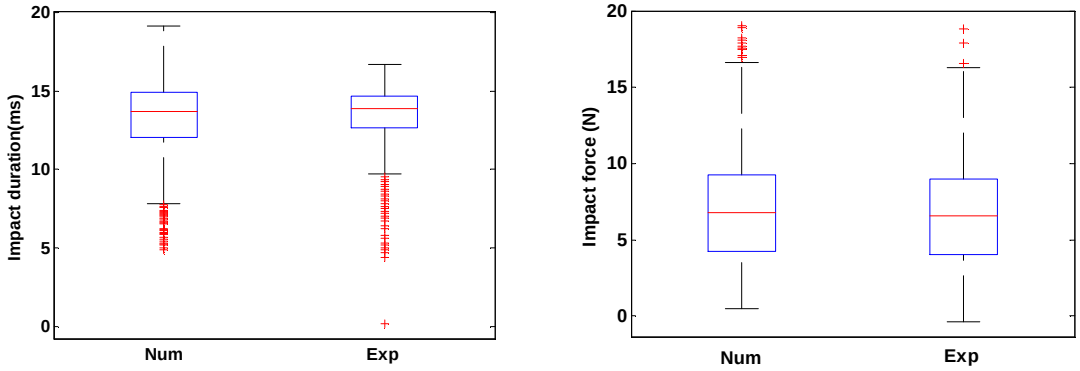

Figure 14: Impact durations and forces for V=2.5m/s & Gain excitation=7 (Num VS Exp)

The impact duration in figure 14 shows that the numerical results are little more scattered than the experimental ones. These differences might be due to the conservative modeling of the gap stops (impact damping was neglected in simulations). This aspect needs more investigations, but globally a good correlation between modeling and measurements was found.

Concerning the impact forces, we observe a good agreement of medians, the first and the third quartiles. Even outliers are well located. Furthermore, the impact force maxima and impact occurrences are still well estimated as shown in the table 3.

	Num	**Exp**	**Err%**
Fmax	18,67	18,8	0,7
Occurrences	1250	1323	5,5
Mean duration (ms)	12,9	13,8	6

Table 3: Comparison between experimental and numerical results (V=2.5m/s for Gain excitation=7)

6 Conclusion

This paper presents a hybrid test method to simulate the fluid-elastic effect on steam generator tubes by using active vibration control technics. This hybrid approach aims to reduce the cost of experiments under real conditions, which might be very expensive and difficult to perform. Among several fluid-elastic models, we have chosen Piteau et al [1] one, in which the fluid-elastic efforts are projected only on the first mode shape.

First, we created a model of the experimental setup. Then we designed two controllers acting separately on modal frequency and modal damping. Combining these two controllers allowed us reproducing the fluid elastic modal effect on the tube, including vortex shedding and fluid elastic instabilities. In the end, we added gap stops to reproduce impacts and study their effect on tube dynamics.

This work also indicates that the impact forces and duration can be estimated numerically especially in lower level of excitation. In cases of higher excitation, the numerical modeling must be more precise and deserves more investigations. However, it gives a good estimation of the tube response.

References

[1] P. Piteau, X. Delaune, J. Antunes, et L. Borsoi, « Experiments and computations of a loosely supported tube in a rigid bundle subjected to single-phase flow », *Journal of Fluids and Structures*, vol. 28, p. 56‑71, janv. 2012.

[2] H. Tanaka et S. Takahara, « Fluid elastic vibration of tube array in cross flow », *Journal of Sound and Vibration*, vol. 77, nº 1, p. 19‑37, juill. 1981.

[3] M. P. Païdoussis, « Fluidelastic vibration of cylinder arrays in axial and cross flow: State of the art », *Journal of Sound and Vibration*, vol. 76, nº 3, p. 329‑360, juin 1981.

[4] D. Weaver, « Some thoughts on the elusive mechanism of fluidelastic instability in heat exchanger tube arrays », presented at the 9th International Conference on Flow-Induced Vibrations, Prague, Czech Republic, 2008, p. 21‑28.

[5] A. J. Fricker, « Numerical analysis of the fluidelastic vibration of a steam generator tube with loose supports », *Journal of Fluids and Structures*, vol. 6, nº 1, p. 85‑107, janv. 1992.

[6] S. O. Rice, *Mathematical analysis of random noise*. Bell Telephone Laboratories, 1944.